# Epitaxial InAs-coupled superconducting junctions


doi: 10.1063/1.343594

# Epitaxial InAs-coupled superconducting junctions

Tatsushi Akazaki, Tsuyoshi Kawakami, and Junsaku Nitta
*Electrical Communications Laboratories, Nippon Telegraph and Telephone Corporation, 3-9-11 Musashino-shi, Tokyo 180, Japan*

(Received 20 July 1989; accepted for publication 15 August 1989)

Homoepitaxial *n*-type InAs-coupled superconducting junctions are investigated. The *n*-type channel layer on a *p*-type substrate has nearly the same mobility as bulk crystal and the layer can be isolated electrically from the substrate by the built-in potential at the *p*-*n* interface. As a result, the critical current-normal resistance ($I_C R_N$) product of the homoepitaxial *n*-type InAs-coupled junction is at least 30 times better than those of the bulk *n*-type ones. The coherence length $\xi_N$ is calculated using the experimentally obtained carrier concentration, mobility, and effective mass. Temperature dependence of $I_C$ agrees with calculations based on the proximity effect theory which can be applied to the intermediate regime between the clean and dirty limits.

## I. INTRODUCTION

Recently semiconductor-coupled superconducting junctions using the superconducting proximity effect have been investigated[1-10] as a step towards superconducting transistors. The most important quantity in the proximity effect is the coherence length in the normal metal, which corresponds to the decay length of the pair potential. The coherence length depends on the relation between the mean free path and the thermal diffusion length of the normal metal. In the dirty limit case where the thermal diffusion length is much longer than the mean-free path, de Gennes and Werthamer[11,12] has shown the coherence length depends on the diffusion constant of the normal metal. Seto and Van Duzer[13] has applied the de Gennes–Werthamer theory to the semiconductor-coupled superconducting junctions. On the other hand, the clean limit cases where the mean-free path is much longer than the thermal diffusion length have been investigated theoretically and experimentally.[14-16] However, the intermediate case between the dirty and clean limits has not been well studied. Recently, Tanaka and Tsukada[17] have proposed the theory of the proximity effect which bridges over the two limits of the dirty and clean system by using Green's function method. The purpose of this paper is to clarify the intermediate case experimentally.

In our previous paper[4] for bulk *n*-type InAs-coupled junction, the experimentally obtained coherence length from the temperature dependence of critical current $I_C$ has differed from the calculated value based on the Seto–Van Duzer theory. This fact suggests that the mean-free path of the bulk *n*-type InAs is comparable to the thermal diffusion length, and the dirty limit case is no longer applied to the junction. However, the $I_C$ for bulk *n*-type InAs-coupled junction cannot be exactly determined near the critical temperature. This is because the normal resistance $R_N$ is very small due to the leakage current into the substrate.

This paper reports on a homoepitaxial *n*-type InAs-coupled superconducting junction. Here, this junction offers a low leakage current, because the built-in potential in the *p*-*n* junction isolates the channel layer from the substrate. As a result, the critical current-normal resistance $I_C R_N$ product is improved and the $I_C$ near the critical temperature can be exactly measured. Moreover, homoepitaxial growth of the channel layer provides high electron mobility close to that of the bulk *n*-type InAs, in contrast to the heteroepitaxial *n*-type InAs.[8] The coherence length can be estimated, based on experimentally obtained values of carrier concentration, mobility, and effective mass. Therefore, the experimentally obtained temperature dependence of $I_C$ can be exactly compared with the dirty, clean, and intermediate case. The present experiment clearly shows that the coherence length is described by the intermediate regime where the mean-free path is comparable to the thermal diffusion length.

## II. EXPERIMENT AND DISCUSSION

### A. Homoepitaxial InAs growth

Homoepitaxial InAs layers were grown by molecular-beam epitaxy (MBE) on (100)-oriented *p*-type InAs (Zn-doped) substrates. Elemental 99.9999% In and 99.99999% $As_4$ source materials were used. Si and Be were used as the *n*-type and *p*-type dopants. The InAs substrates were etched in HBr:3% Br-methanol:$H_2O$ solution (2:1:1), rinsed in the deionized distilled water and blown to dry with pure nitrogen before being indium-soldered onto the Mo heating block. Prior to the epitaxial layer deposition, the substrates were heated in vacuum at 500 °C for 10–20 min in an arsenic flux to reduce surface contamination and to reconstruct the surface crystallinity. The surface structures of the substrate were monitored by reflection high energy electron diffraction (RHEED) prior to epitaxial layer growth. The epitaxial layer was monitored by RHEED during and after growth. The homoepitaxial structure consisted of an *n*-type InAs channel layer (0.2–1.0 $\mu$m thick) and a *p*-type InAs buffer layer (1.0 $\mu$m thick) on a *p*-type InAs substrate. The *p*-type InAs buffer layer was made in order to eliminate the effect of defects and Zn interdiffusion, which was estimated to have a diffusion length of about 0.1 $\mu$m from the InAs substrate by secondary-ion mass spectroscopy (SIMS). The InAs layers were deposited at growth rates of 0.6 to 1.3 $\mu$m/h at growth temperatures in the range 430 to 480 °C, with $As_4$:In flux ratios varying from 20:1 to 50:1. Films

 0021-8979/89/246121-05$02.40  

grown under these conditions were mirrorlike with few surface defects.

### B. Comparison of *I-V* characteristics

The structure of a homoepitaxial *n*-type InAs-coupled superconducting junction is illustrated in Fig. 1. Nb electrodes were patterned by a lift-off technique. First, a resist for the Nb electrodes was patterned by electron-beam lithography. Then, the ridge structure of InAs, which forms a superconducting channel, was formed by shallow etching. After Ar sputter cleaning at the InAs surface, Nb was deposited at an angle from both directions of the ridge. The final process was lift-off. The 110-nm-thick Nb electrodes have a $T_C$ of 9.0 K, the length $L$ between Nb electrodes is 0.36 $\mu$m, the width $W$ is 80 $\mu$m, and the thickness $d$ of the *n*-type InAs channel layer is 0.35 $\mu$m in the junction of sample 1.

The *I-V* characteristics of the homoepitaxial *n*-type InAs-coupled junction are compared with those of the bulk *n*-type InAs-coupled junction at 2.0 K in Fig. 2. Table I shows junction properties using homoepitaxial *n*-type and bulk *n*-type InAs substrates. The results clearly show that $R_N$ and the $I_C R_N$ product of the homoepitaxial *n*-type InAs-coupled junction are at least 30 times as large as those of the bulk *n*-type InAs-coupled junctions. However, this qualitative comparison is not very meaningful due to the difference in the mobilities and the carrier concentrations of the two different types of junction. This fact suggests that the leakage current remarkably decreases, and that the current only flows into the *n*-type InAs-channel layer. It is thought that the good isolation resulted from the built-in potential in the *p-n* junction.

### C. Coherence length

According to the proximity effect theory,[11] a pair potential is induced in the normal metal of a superconductor/normal ($S/N$) sandwich system. The most important quantity

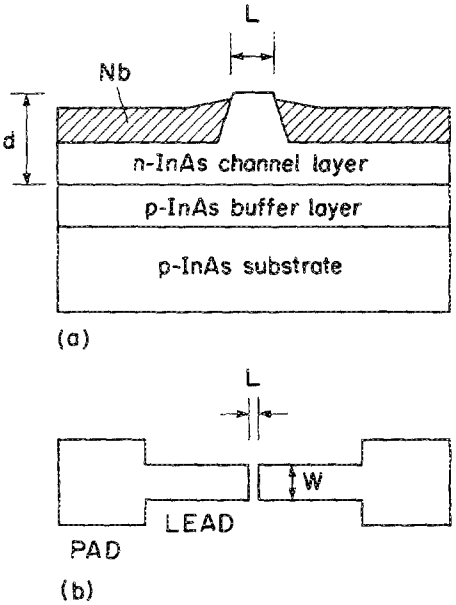


FIG. 1. Schematic of the fabricated junction structure. (a) Cross-sectional view and (b) electrode configuration.

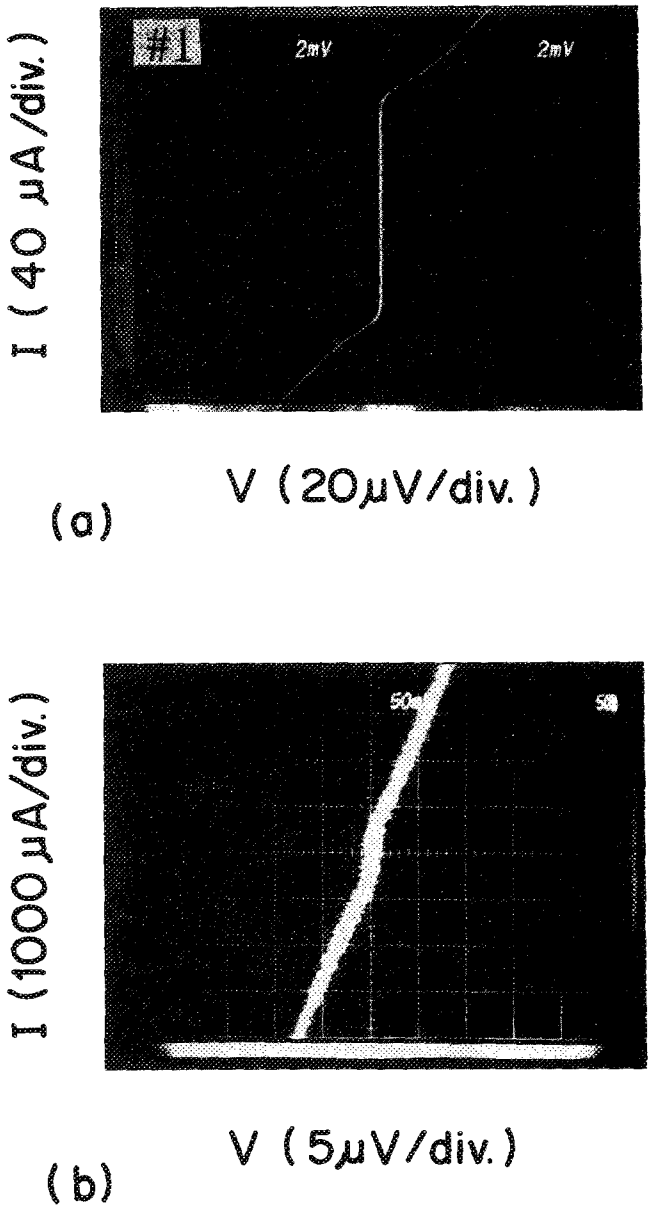


FIG. 2. Comparison of dc *I-V* characteristics between the homoepitaxial and bulk *n*-type InAs-coupled junctions at 2.0 K. (a) Junction using homoepitaxial *n*-type InAs with carrier concentration $n$ of $1.5\times10^{17}$ cm$^{-3}$, length $L$ of 0.36 $\mu$m between Nb electrodes, and width $W$ of 80 $\mu$m. (b) Junction using bulk *n*-type InAs with $n = 2.3\times10^{18}$ cm$^{-3}$, $L = 0.24$ $\mu$m, and $W = 80$ $\mu$m.

TABLE I. Junction properties using homoepitaxial *n*-type InAs and bulk *n*-type InAs substrates at 2.0 K. $L$, $d$, $n$, $\mu$, $I_C$, $R_N$, and $I_C R_N$ are defined in the text.

| | Homoepitaxial (sample 1) | | Bulk | |
|---|---|---|---|---|
| $L(\mu m)$ | 0.36 | 0.24 | 0.51 | 0.51 |
| $d(\mu m)$ | 0.35 | ... | ... | ... |
| $n(cm^{-3})$ | $1.5\times10^{17}$ | $2.6\times10^{18}$ | $2.5\times10^{17}$ | $2.4\times10^{16}$ |
| $\mu(cm^2/V\,s)$ | $2.1\times10^{4}$ | $1.0\times10^{4}$ | $1.7\times10^{4}$ | $2.5\times10^{4}$ |
| $I_C(\mu A)$ | 109.8 | 600 | 46 | 5.3 |
| $R_N(\Omega)$ | 0.361 | 0.0021 | 0.0125 | 0.13 |
| $I_C R_N$(mV) | 0.0396 | 0.0013 | 0.0006 | 0.0007 |

in this system is the coherence length in the normal metal $\xi_N$. The expression for $\xi_N$ depends on the ratio of the mean-free path $l = v_F\tau$ and the thermal diffusion length $L_T = (\hbar D/k_B T)^{1/2}$, where $v_F$ is the Fermi velocity, $\tau$ is the relaxation time, and $D$ is the diffusion coefficient in the normal metal. In the dirty limit, where $l \ll L_T$, the coherence length is expressed as[11]

$$\xi_N(T) = (\hbar^3\mu/6\pi k_B T e m^*)^{1/2}(3\pi^2 n)^{1/3}, \quad l \ll L_T. \tag{1}$$

In the clean limit case, where $l \gg L_T$, the coherence length is expressed as[15,16]

$$\xi_N(T) = (\hbar/2\sqrt{3}\pi k_B T m^*)(3\pi^2 n)^{1/3}, \quad l \gg L_T. \tag{2}$$

Recently, Tanaka and Tsukada[17] introduced a coherence length for the general case using Green's function method. Here, the coherence length can be applied to the intermediate case, where $l$ is comparable to $L_T$, and is given by

$$\xi_N(T) = [\hbar^3\mu/6\pi k_B T e m^*(1 + 2\pi k_B T\tau/\hbar)]^{1/2}(3\pi^2 n)^{1/3}. \tag{3}$$

The induced pair potential $\Delta_N$ at the $S/N$ boundary exponentially decays in the normal metal if $L > \xi_N$ holds, and is given by

$$\Delta_N(X) \propto \exp(-X/\xi_N). \tag{4}$$

The above equation can be applied to the clean limit as well as to the dirty limit.[16] Therefore, the critical current is described as

$$I_C \propto \left[\frac{\Delta_N(0)}{\cosh\left(\frac{L}{2\xi_N}\right)}\right]^2 \frac{1}{\xi_N}, \tag{5}$$

as in the equation proposed by Seto and Van Duzer.[13]

### D. Transport properties of epitaxial *n*-type InAs layers

As has been shown, the coherence length of the *n*-type InAs-channel layer in the superconducting proximity effect system depends on the carrier concentration $n$, the mobility $\mu$, and the effective mass $m^*$. To compare the experiment with the theory, these values must be determined. Here, $n$, $\mu$, and $m^*$ are determined from the magnetic transport properties. First, the mobility was estimated from magnetoresistance measurements. Resistivity was measured by the standard four-probe method with Au corbino electrodes. The Au electrodes were made by evaporating Au with a lift-off technique after Ar sputter cleaning. The Au electrodes had a corbino-disk structure with an inner diameter 150 $\mu$m and an outer diameter 350 $\mu$m. The resistance values of sample 1 were proportional to the square of the magnetic field at 3 K as shown in Fig. 3. The mobility was estimated to be $2.1\times10^4$ cm$^2$/V s at 3 K using the corbino-magnetoresistance expression: $\Delta R(B)/R(0) = 1 + \mu^2B^2$ up to 0.5 T.[18] This magnetoresistance mobility agrees very well with the calculated one of $2.2\times10^4$ cm$^2$/V s using the resistivity and the carrier concentration, obtained from the period of Shubnikov–de Haas (SdH) oscillation. This result shows that the magnetoresistance mobility is equal to the drift mobility of InAs.

The carrier concentration and the effective mass can be determined by analyzing the SdH oscillations. The period

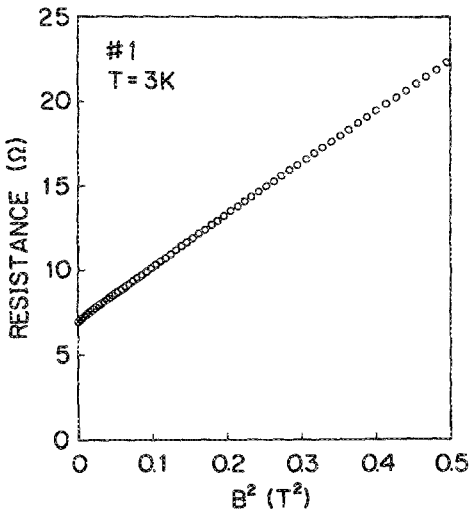


FIG. 3. Variation in the resistivity as a function of the square of the magnetic field at 3 K.

and temperature dependence of SdH oscillations are related to the carrier concentration and the effective mass, respectively. The SdH oscillations were measured up to 5 T in the temperature range of 3–70 K. Figure 4 shows the SdH oscillatory components of sample 1 extracted from the magnetoresistance as a function of inverse magnetic field. The oscillation of the magnetoresistance is periodic. The carrier concentration $n$ for the *n*-type InAs layer was estimated to be $1.5\times10^{17}$ cm$^{-3}$ using $n = [2e/\hbar\Delta(1/B)]^{3/2}/3\pi^2$, where $\Delta(1/B)$ is the period of the SdH oscillation. Figure 5 shows the temperature dependence of SdH oscillatory component amplitudes for sample 1 at 3.81 T. The effective mass $m^*$ was determined by fitting the experimental data to the theoretical equation expressed by

$$\Delta R(B) \propto T/\sinh(2\pi^2 k_B T m^*/e\hbar B), \tag{6}$$

which is valid in the range of sinusoidal oscillations. The best

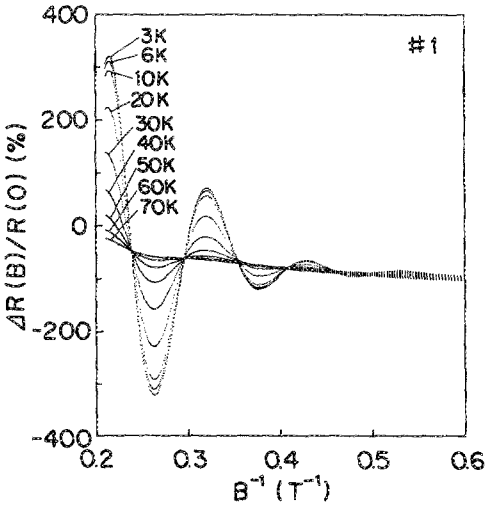


FIG. 4. Shubnikov–de Haas (SdH) oscillatory components for a homoepitaxial *n*-type InAs film as a function of inverse magnetic field at 3–70 K.

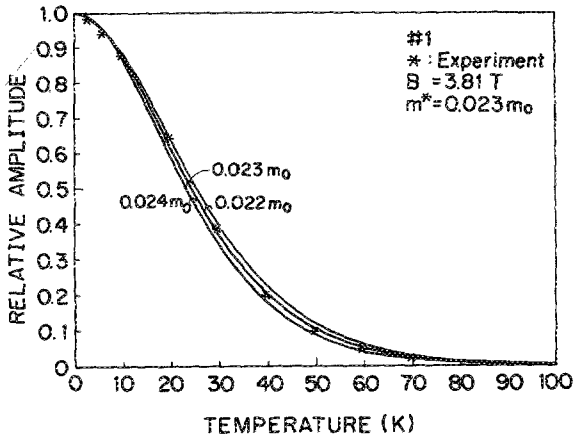


FIG. 5. Temperature dependence of SdH oscillatory component amplitudes at 3.81 T. The solid lines represent the theoretical curves using $m^* = 0.022m_0$, $0.023m_0$, and $0.024m_0$, respectively.

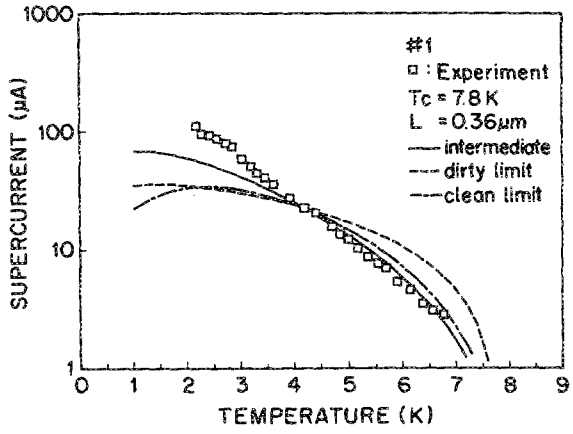


FIG. 7. Theoretical fitting of experimental data for $I_C$. Calculations are made for three cases of the proximity effect theory.

fit value was given by $m^* = 0.023\ m_0$, where $m_0$ is the free-electron mass.

Figure 6 compares the carrier-concentration dependence of mobilities between several samples of epitaxial $n$-type InAs and bulk $n$-type InAs. The transport properties of the homoepitaxial $n$-type InAs were confirmed to be nearly the same as bulk $n$-type InAs, in contrast to the heteroepitaxial $n$-type InAs. The low mobility of heteroepitaxial $n$-type InAs is possibly due to the lattice mismatch between GaAs and InAs.

The coherence length can be estimated, based on these experimentally obtained values of $n$, $\mu$, and $m^*$. The experimentally obtained temperature dependence of $I_C$ can be qualitatively compared with the theory.

### E. Comparison between the theory and the experiment

The mean free path $l$ and the thermal diffusion length $L_T$ for the homoepitaxial $n$-type InAs channel layer were estimated to be 0.23 and 0.34 $\mu$m, respectively, using the values of $n = 1.5\times10^{17}$ cm$^{-3}$, $\mu = 2.1\times10^{4}$ cm$^2$/V s, $m^* = 0.023\,m_0$, and $T = 4.2$ K for sample 1. This estimation suggests that neither the dirty ($l \ll L_T$) nor clean limit ($l \gg L_T$) of the proximity effect theory can be applied to the present $n$-type InAs-coupled superconducting junction.

The temperature dependence of $I_C$ was measured for the junction of sample 1. Figure 7 compares the experimental results with each of the three theoretical ones. For the absolute value of $I_C$, the theoretical expression in Eq. (5) cannot provide a reasonable estimate because the boundary condition of an $S/N$ interface is crucial and is not determined completely. Here, to avoid the problem, $I_C$ theoretically obtained from Eq. (5) is normalized against the experimentally obtained one of 4.2 K. Of these three $I_C - T$ characteristics, the intermediate case agrees with experimental results as expected. The coherence length $\xi_N$ was estimated to be 0.16 $\mu$m at 2.0 K in the intermediate regime. In the homoepitaxial $n$-type InAs-coupled junction, the mean-free path is comparable to the thermal diffusion length because of the high-electron mobility. Consequently, the dirty limit case no longer applies to this junction.

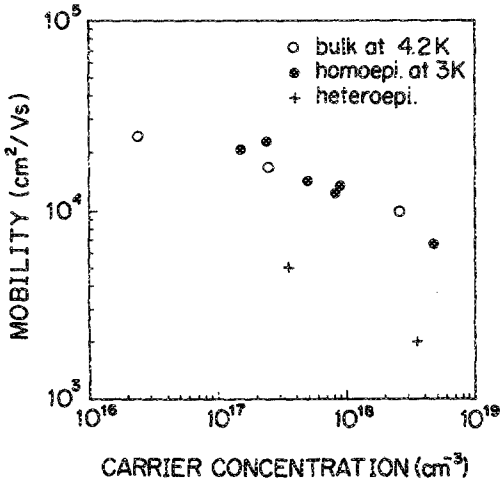


FIG. 6. Carrier concentration vs mobility plot for homoepitaxial $n$-type InAs films, compared with bulk and heteroepitaxial $n$-type InAs. The data for heteroepitaxial $n$-type InAs are taken from Ref. 8.

## III. CONCLUSION

In a superconducting junction with a homoepitaxial $n$-type InAs thin film acting as the channel layer on a $p$-type substrate, the mobility of the film is nearly the same as that of bulk $n$-type InAs. Good isolation of the channel layer from the substrate was achieved by the built-in potential in the $p$-$n$ junction. The $I_C R_N$ product of the homoepitaxial $n$-type InAs junctions was at least 30 times as large as that of the bulk $n$-type InAs junctions due to the decrease in the leakage current. The effective mass determined by SdH oscillation is $0.023m_0$ for a carrier concentration of $1.5\times10^{17}$ cm$^{-3}$. The good agreement between the experimental results and the theoretical ones shows that the present system can be consistently described by the intermediate regime using the proximity effect theory.

## ACKNOWLEDGMENTS

The authors would like to thank Professor Masaru Tsukada and Dr. Yukio Tanaka for their valuable discussions and comments. They also express their thanks to Dr. Hiroshi Okamoto, Dr. Tomoaki Yamada, and Azusa Matsuda for their continuous support; to Dr. Hideaki Takayanagi, and Koh Inoue for their kind advice, and to Takehisa Kawashima for his electron-beam lithography.

[1]T. D. Clark, R. J. Prance, and A. D. C. Grassie, J. Appl. Phys. **51**, 2736 (1980).
[2]A. H. Silver, A. B. Chase, M. McColl, and M. F. Millea, *AIP Conference Proceedings 44: Future Trends in Superconductive Electronics* (AIP, New York, 1978), p 364.
[3]R. C. Ruby and T. Van Duzer, IEEE Trans. Electron Devices **ED-28**, 1394 (1981).
[4]T. Kawakami and H. Takayanagi, Appl. Phys. Lett. **46**, 92 (1985).
[5]H. Takayanagi and T. Kawakami, Phys. Rev. Lett. **54**, 2449 (1985).
[6]T. Nishino, M. Miyake, Y. Harada, and U. Kawabe, IEEE Electron Device Lett. **EDL-6**, 297 (1985).
[7]T. Nishino, E. Yamada, and U. Kawabe, Phys. Rev. B **33**, 2042 (1986).
[8]A. W. Kleinsasser, T. N. Jackson, G. D. Pettit, H. Schmid, J. M. Woodall, and D. P. Kern, Appl. Phys. Lett. **49**, 1741 (1986).
[9]Z. Ivanov, T. Cleason, and T. Andersson, Jpn. J. Appl. Phys. **26**, Suppl. 26-3, 1617 (1987).
[10]T. Kawakami, T. Akazaki, and K. Inoue, *Extended Abstracts of the 1987 International Superconductivity Electronics Conference*, ISEC '87 (JSAP, Tokyo, 1987), p. 174.
[11]P. G. de Gennes, Rev. Mod. Phys. **36**, 225 (1964); *Superconductivity of Metals and Alloys* (Benjamin, New York, 1969).
[12]N. R. Werthamer, Phys. Rev. **132**, 2440 (1963).
[13]J. Seto and T. Van Duzer, in *Low Temperature Physics LT-13*, edited by K. D. Timmerhous, W. J. O'Sullivan, and E. F. Hammel (Plenum, New York, 1974), Vol. 3, p. 328.
[14]W. L. McMillan, Phys. Rev. **175**, 537 (1968).
[15]Y. Krahenbuhl and R. J. Watts-Tobin, J. Low Temp. Phys. **35**, 569 (1979).
[16]T. Y. Hsiang and D. K. Finnemore, Phys. Rev. B **22**, 154 (1980).
[17]Y. Tanaka and M. Tsukada, Phys. Rev. B **37**, 5087 (1988).
[18]E. Yamaguchi, Phys. Rev. B **32**, 5280 (1985).